

Efficient ground state preparation in variational quantum eigensolver with symmetry breaking layers

Chae-Yeun Park

Institute for Theoretical Physics, University of Cologne, 50937 Köln, Germany

Variational quantum eigensolver (VQE) that solves the ground state of a Hamiltonian is a promising application of noisy intermediate-scale quantum devices. The quantum alternating operator Ansatz (QAOA) is one of the most widely studied Ansätze for this purpose and solves many Hamiltonians reliably. However, because of inherited symmetries from the Hamiltonian, the QAOA is not necessarily good at solving problems with symmetry broken nature. In this paper, we propose a variational Ansatz with symmetry breaking layers for solving those systems. Notably, our Ansatz finds a constant-depth circuit for solving a symmetry broken ground state which is impossible for the QAOA. We also propose a simple learning technique that can choose a particular symmetry broken state among degenerate ground states.

I. INTRODUCTION

Experimental progress in controlling quantum systems has allowed the first demonstration of quantum computational advantage [1] in the recent years, and a noisy quantum device with hundreds of qubits is getting visible. Those devices, which are often dubbed as noisy intermediate-scale quantum (NISQ) [2] computers, are expected to solve a practical computational problem beyond the reach of classical computers. Among possible applications, variational quantum eigensolver (VQE) [3, 4] that solves the ground state problem of quantum many-body Hamiltonian has gained lots of attention recently (see Ref. [5] for a recent review).

The VQE works by combining a parameterized quantum circuit and a classical optimization algorithm: A quantum circuit evaluates the expectation value of the Hamiltonian and its derivatives for the output quantum state, whereas a classical optimizer finds better parameters that minimize the energy. As solving the ground state of quantum Hamiltonians are difficult for classical computers, one may easily get an advantage of VQEs. Still, it is unclear which Ansatz and classical optimizer should be used to efficiently solve a given Hamiltonian.

One of the most widely studied Ansätze for solving translational invariant many-body Hamiltonians is the quantum alternating operator Ansatz (QAOA) [6]. Inspired by a short-depth quantum algorithm for solving combinatorial optimization problems [7], this Ansatz is composed of rotating gates using the terms of the Hamiltonian. Even though the QAOA solves many different Hamiltonians reliably [8–10], however, it is not necessarily good at solving problems with symmetry broken nature which prevail in many-body systems. Indeed, there are local Hamiltonians whose ground states cannot be generated by this Ansatz in constant-depth albeit such a circuit exists, as the circuit obeys the same symmetry as the Hamiltonian [11].

In this paper, we devise a symmetry breaking Ansatz and explore its power for solving many-body Hamiltonians. We first show that our Ansatz can generate a ground state within a different symmetry protected sector than

the input state in constant-depth, which is impossible for the bare QAOA. We next use our symmetry breaking Ansatz to prepare a particular symmetry broken state among degenerate ground states. This is done by simply adding a symmetry penalizing term to the loss function.

II. SYMMETRY BREAKING ANSATZ

The first model we study is the transverse field Ising (TFI) model for N qubits defined by the Hamiltonian

$$H_{\text{TFI}} = - \sum_{i=1}^N Z_i Z_{i+1} - h \sum_{i=1}^N X_i \quad (1)$$

where we impose the periodic boundary condition $Z_{N+1} = Z_1$. This model has two distinct (ferromagnetic and paramagnetic) phases depending on the strength of h that are protected by the spin flip symmetry $P = \prod_i X_i$ [12]. The critical point of this model $h = 1$ is well known. This implies that if there is a circuit that commutes with P and connects two ground states in different phases, then the circuit depth must be larger than a constant [13]. On the other hand, there is a finite-depth circuit that connects two different ground states if we do not restrict to such a symmetry, as the system is gapped unless $h = 1$ [13, 14].

As a common Ansatz for preparing the ground state only utilizes terms within the Hamiltonian, it fails to represent such a circuit. For example, the QAOA Ansatz for this Hamiltonian is given by $\prod_{k=D}^1 L_x(\phi_k) L_{zz}^{\text{odd}}(\kappa_k) L_{zz}^{\text{even}}(\vartheta_k) |+\rangle^{\otimes N}$ where $L_x(\phi) = \exp[-i\phi \sum_i X_i]$, $L_{zz}^{\text{odd}}(\kappa) = \exp[-i\kappa \sum_{i=1}^{N/2} Z_{2i-1} Z_{2i}]$, and $L_{zz}^{\text{even}}(\vartheta) = \exp[-i\vartheta \sum_{i=1}^{N/2} Z_{2i} Z_{2i+1}]$. As all gates commute with P , i.e. $[P, L_{zz}^{\text{odd}}] = [P, L_{zz}^{\text{even}}] = [P, L_x] = 0$, and the input state $|+\rangle^{\otimes N}$ is the ground state of the Hamiltonian when $h \rightarrow \infty$, we know that preparing the ground state for $h < 1$ requires circuit depth larger than a constant. Indeed, theoretical and numerical studies have found that this type of Ansatz needs depth $D \geq N/2$ to prepare the ground state faithfully [8, 15].

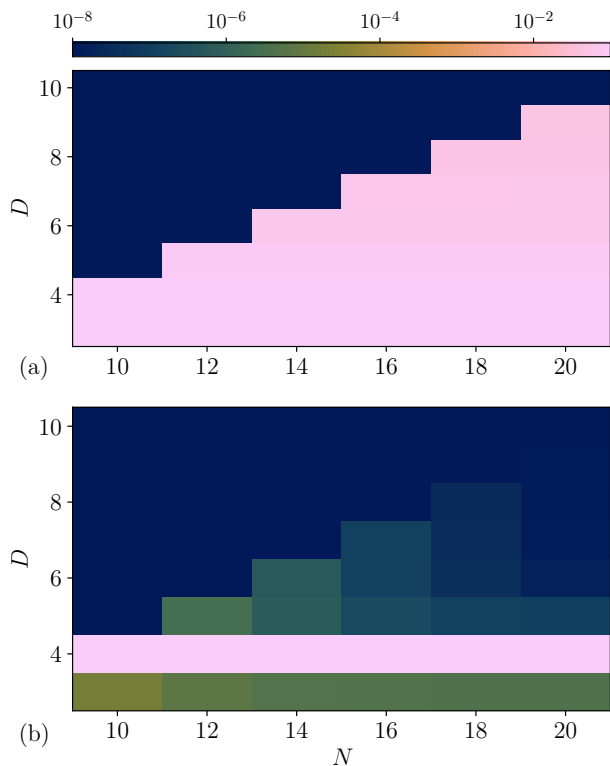


Figure 1. Converged normalized energy $\tilde{E} = (E_{\text{VQE}} - E_{\text{GS}})/E_{\text{GS}}$ as a function of system size N and circuit depth D (a) without and (b) with symmetry breaking layers for the transverse field Ising (TFI) model where E_{GS} is the true ground state energy. We have run 12 independent VQE runs and taken the best optimized energy for each N and D . Initial parameters are sampled randomly from the normal distribution $\mathcal{N}(0, \sigma^2)$ besides $D = 3, 5$ at (b) where we have added $2\pi/D$ to the parameters of the symmetry breaking layers (see main text for details).

We now add symmetry breaking layers in VQE Ansatz and see whether it can achieve lower circuit depth for preparing the ground state. Our Ansatz for the TFI is given as

$$|\psi(\boldsymbol{\theta})\rangle = \prod_{j=D}^1 L_z(\phi_j) L_x(\kappa_j) L_{zz}(\vartheta_j) |+\rangle^{\otimes N} \quad (2)$$

where $L_{zz}(\theta_j) = \exp[-i\theta_j \sum_i Z_i Z_{i+1}]$, $L_x(\kappa_j) = \exp[-i\kappa_j \sum_i X_i]$, $L_z(\phi_j) = \exp[-i\phi_j \sum_i Z_i]$, and $\boldsymbol{\theta} = \{\vartheta_j, \kappa_j, \phi_j\}_{j=1}^D$ is a set of all parameters. All layers in the Ansatz preserve the translational symmetry but the $L_z(\phi_j)$ layers break the symmetry P of the Hamiltonian.

To observe the effect of symmetry breaking layers, we first present the relative errors for different system sizes, depths, with and without the symmetry breaking $L_z(\phi_j)$ layers. We optimize parameters using the quantum natural gradient [16–18]: For each epoch t , we update parameters as $\boldsymbol{\theta}_{t+1} = \boldsymbol{\theta}_t - \eta(\mathcal{F} + \lambda_t \mathbb{1})^{-1} \nabla_{\boldsymbol{\theta}} \langle \psi(\boldsymbol{\theta}_t) | H | \psi(\boldsymbol{\theta}_t) \rangle$ where η is the learning rate, $\mathcal{F} = (\mathcal{F}_{ij})$ is the quantum Fisher matrix, and λ_t is

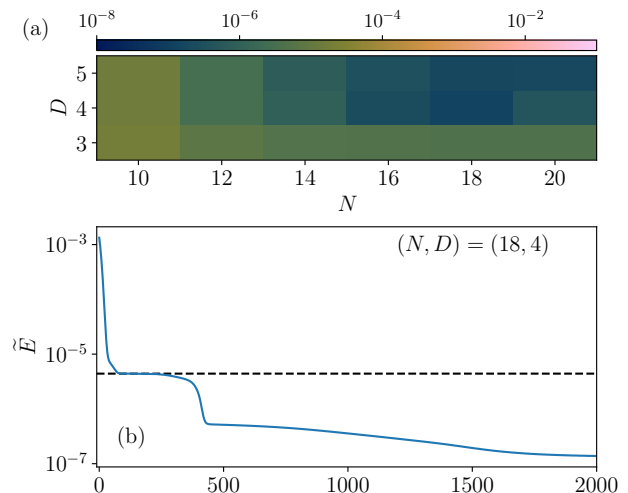


Figure 2. (a) Converged normalized energies \tilde{E} for system size N and circuit depth D (a) from the transfer learning. Results for $D = 3$ is from the random initialization (which are shown in Fig. 1). For $D = 4$, we have trained a circuit after adding a randomly initialized block in the middle of the converged circuit from $D = 3$ (for the same N). Likewise, we obtained results for $D = 5$ using the converged circuits from $D = 4$. (b) A learning curve from the transfer learning when $(N, D) = (18, 4)$. The dashed line indicates the converged energy from $(N, D) = (18, 3)$.

a (step dependent) regularization constant. We choose this optimizer as it works more reliably in solving the ground problem both for classical neural networks [19] and VQEs [9]. For the quantum Fisher matrix, we use the centered one $\mathcal{F} = \mathcal{F}_{ij}^c = \Re\{\langle \partial_{\theta_i} \psi(\boldsymbol{\theta}_t) | \partial_{\theta_j} \psi(\boldsymbol{\theta}_t) \rangle - \langle \partial_{\theta_i} \psi(\boldsymbol{\theta}_t) | \psi(\boldsymbol{\theta}_t) \rangle \langle \psi(\boldsymbol{\theta}_t) | \partial_{\theta_j} \psi(\boldsymbol{\theta}_t) \rangle\}$ [17] mostly (unless otherwise stated), but the uncentered one $\mathcal{F}_{ij}^{\text{nc}} = \Re\{\langle \partial_{\theta_i} \psi(\boldsymbol{\theta}_t) | \partial_{\theta_j} \psi(\boldsymbol{\theta}_t) \rangle\}$ [16] is also considered when it improves the performance. The difference between two can be understood using the notion of the projected Hilbert space [18]. For the hyperparameters, we typically use $\eta = 0.01$ and $\lambda_t = \max(100.0 \times 0.9^t, 10^{-3})$.

We show the optimized normalized energies $\tilde{E} = (E_{\text{VQE}} - E_{\text{GS}})/E_{\text{GS}}$ for different N and D in Fig. 1 when $h = 0.5$. We have used the Fisher matrix with the centering term \mathcal{F}^c and initial values of parameters $\{\vartheta_j, \kappa_j, \phi_j\}$ are sampled from the normal distribution $\mathcal{N}(0, \sigma^2)$ with $\sigma = 0.001$ besides $D = 3, 5$ at Fig. 1(b). When $D = 3$ (all N) and 5 (for $N \geq 12$), this initialization does not give any better energy than the Ansatz without symmetry breaking layers. We instead found that initializing parameters for the symmetry breaking layers $\{\phi_j\}$ with samples from $\mathcal{N}(2\pi/D, \sigma^2)$ finds better optima in these cases. However, this initialization does not change the results for $D = 4$, and performs even worse when $D \geq 6$ (see Appendix A for detail comparisons).

Fig. 1(a) shows that the ground state is only found for $D \geq N/2$ when symmetry breaking layers are absent, which is consistent with Refs. [8, 9]. On the other

hand, results with symmetry breaking layers [Fig. 1(b)] clearly demonstrate that converged energies are significantly improved for $5 \leq D < N/2$. Most importantly, converged normalized energies are $\leq 10^{-7}$ for all N when $D \geq 9$, which implies that our Ansatz finds a constant-depth circuit for solving the ground state. In addition, the results show that there is a finite-size effect up to $N = 18$ where the accurate ground state is only obtained when $D \geq N/2$.

However, there is a huge gap between the converged energies and the true ground state when $D = 4$. In fact, the results for $D = 4$ are even worse than those of $D = 3$, which signals that the optimizer gets stuck in local minima. This type of convergence problem is already observed in Ref. [9]. To obtain a better convergence for $D = 4$, we employ a transfer learning technique. Instead of starting from a randomly initialized circuit, we insert a block in the middle of the converged circuit from $D = 3$ and perturb all parameters by adding small numbers sampled from $\mathcal{N}(0, \sigma'^2)$ (where we typically use $\sigma' = 0.01$). We then optimize the full circuit using the quantum natural gradient.

We show converged energies from the transfer learning in Fig. 2. Fig. 2(a) illustrates that the transfer learning succeeds to find a better optima for $D = 4$. However, the result for $(N, D) = (10, 5)$ is worse than that of the random initialization, which implies that the transfer learning does not necessarily find the global optima. We additionally plot a learning curve for $(N, D) = (18, 4)$ in Fig. 2(b) where the initial energy is much higher due to an added perturbation but it eventually finds a lower energy state.

We next consider the transverse field cluster (TFC) model, the Hamiltonian of which is given as

$$H_{\text{TFC}} = - \sum_{i=1}^N Z_i X_{i+1} Z_{i+2} - h \sum_{i=1}^N X_i. \quad (3)$$

It is known that the phase transition of this model also takes place at $h = 1$ [20]. As the terms $Z_i X_{i+1} Z_{i+2}$ are mutually commuting, the ground state at $h = 0$ is the common eigenvector of those operators which is also known as the cluster state. Two relevant symmetries that determine the ground state of this model are $P_1 = \prod_{i=1}^{N/2} X_{2i}$ and $P_2 = \prod_{i=1}^{N/2} X_{2i-1}$ [21, 22]. We thus expect that a circuit cannot bring the product state $|+\rangle^{\otimes N}$ to the ground state of the Hamiltonian when $h < 1$ in a constant depth as long as it commutes with P_1 and P_2 .

We study whether a symmetry breaking layer can improve it. To see this, we construct our Ansatz

$$|\psi(\theta)\rangle = \prod_{j=D}^1 L_z^{\text{even}}(\phi_j) L_z^{\text{odd}}(\chi_j) \times L_x(\kappa_j) L_{zzz}(\theta_j) |+\rangle^{\otimes N} \quad (4)$$

where $L_{zzz}(\theta_j) = \exp[-i\theta_j \sum_{i=1}^N Z_i X_{i+1} Z_{i+2}]$, $L_z^{\text{even/odd}}(\phi_j) = \exp[-i\phi_j \sum_{i=1}^{N/2} Z_{2i/2i+1}]$. Converged

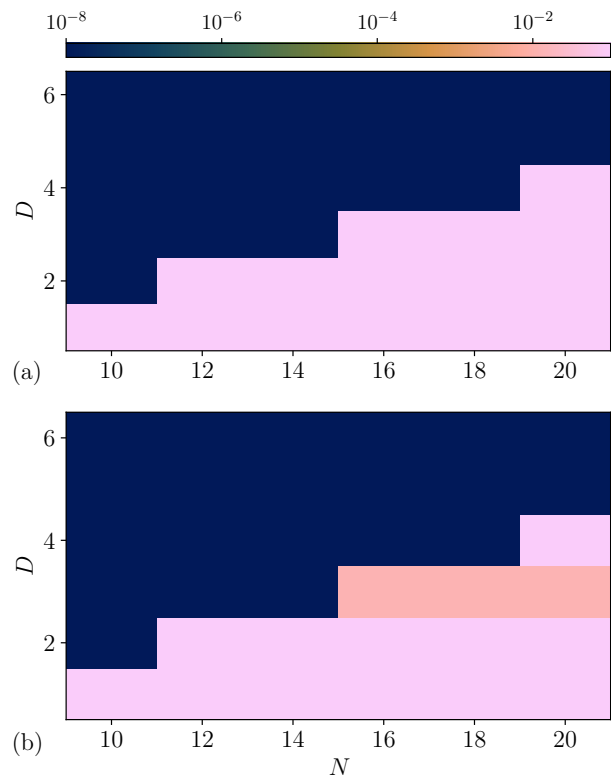


Figure 3. Converged normalized energies \tilde{E} for system size N and circuit depth D (a) without and (b) with symmetry breaking layers for the transverse field Cluster (TFC) model.

normalized energies with and without symmetry breaking layers for $h = 0.5$ are shown in Fig. 3. The results without symmetry breaking layers show that circuits with $D \geq \lfloor N/4 \rfloor$ solve the ground state accurately. However, the symmetry breaking layers only improve the results for $D = 3$ when $N \geq 16$ for this Hamiltonian. In addition, such an improvement is observed only when the uncentered Fisher matrix \mathcal{F}^{uc} and the initial value $2\pi/D$ for symmetry breaking layers are used. We moreover see that our Ansatz does not find a constant-depth circuit for solving the ground state based upon the results up to $N = 20$. We attribute this to the finite-size effect and expect that much larger system size N (which is beyond our computational capacity) is required to find the constant-depth circuit.

III. PREPARING A SYMMETRY BROKEN GROUND STATE

We next consider the cluster Hamiltonian [Eq. (3) with $h = 0$] with the open boundary condition, which is given as

$$H_{\text{cluster}} = - \sum_{i=1}^{N-2} Z_i X_{i+1} Z_{i+2}. \quad (5)$$

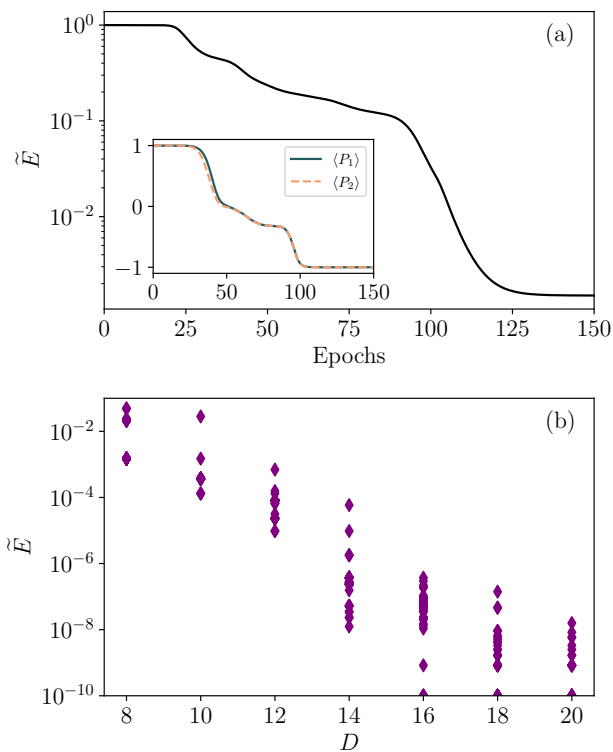


Figure 4. (a) Learning curve of the VQE for preparing the ground state with $\langle P_1 \rangle = \langle P_2 \rangle = -1.0$. A circuit with $(N, D) = (14, 8)$ is used. Inset shows the learning curves for $\langle P_1 \rangle$ and $\langle P_2 \rangle$. (b) Converged normalized energies \tilde{E} for difference circuit depths D . For each D , we show converged energies from 48 independent VQE runs.

Ground states of this model are stabilized by $N-2$ terms ($Z_i X_{i+1} Z_{i+2} |\psi_{\text{GS}}\rangle = |\psi_{\text{GS}}\rangle$ for $i \in [1, \dots, N-2]$), thus 4-fold degenerate. As the operators P_1 and P_2 commute with all stabilizers, they further define the ground state manifold. For the QAOA, the ground state must be +1 eigenstate of P_1 and P_2 as they commute with the circuit and $P_{1,2} |+\rangle^{\otimes N} = +1 |+\rangle^{\otimes N}$. In contrast, we show our Ansatz [Eq. (4)] (with $L_{zzz}(\theta_j)$ in the open boundary condition) can be used to prepare a particular state within the manifold.

The main idea is minimizing the expectation value of $O = H_{\text{cluster}} + \alpha_1 P_1 + \alpha_2 P_2$ for suitable α_1 and α_2 , instead of the Hamiltonian itself. We expect the obtained state is an eigenstate with the corresponding eigenvalue ± 1 of P_i when $\text{sign}(\alpha_i) = \mp 1$.

As an example, we study the VQE for preparing the ground state with $P_1 = P_2 = -1$ using $(N, D) = (14, 8)$. We have tested VQEs with the varying learning rates $\eta \in [0.01, 0.025, 0.05, 0.1]$ and $\alpha_1 = \alpha_2 = \alpha \in$

$[0.1, 0.3, 0.5, 1.0, 2.0, 4.0]$, and found that the desired state can be prepared by the best for $\eta = 0.025$, $\alpha = 2.0$. Especially, all VQE runs have converged to $\langle P_1 \rangle = \langle P_2 \rangle = -1$ (accuracy within 10^{-8}) with these values of η and α . The resulting learning curve is shown in Fig. 4(a). However, the converged energy $\tilde{E} \approx 1.502 \times 10^{-3}$ for $D = 8$ may not be satisfying compared to the other models we have studied above. Thus, we further study whether increasing D helps the convergence in Fig. 4(b). The results show that the converged energies are getting accurate as we increase D . Precisely, 47 instances out of 48 independent VQEs runs have converged to $\tilde{E} \leq 10^{-8}$ when $D = 20$.

ACKNOWLEDGEMENT

The author thanks David Wierichs for helpful discussions. This project was funded by the Deutsche Forschungsgemeinschaft under Germany's Excellence Strategy - Cluster of Excellence Matter and Light for Quantum Computing (ML4Q) EXC 2004/1-390534769 and within the CRC network TR 183 (project grant 277101999) as part of project B01. The numerical simulations were performed on the JUWELS cluster at the Forschungszentrum Juelich. Source codes for the current paper can be found in Github repository [23].

Appendix A: Optimization of the Ansatz with symmetry breaking layers

When the Ansatz contains symmetry breaking layers, an optimization algorithm easily stuck in local minima. We here compare several different set-ups for the transverse field Ising model we have studied in Sec. II. We show results from the transverse Ising model with different initial values and using the centered and uncentered Fisher matrix in Fig. 5. We can see that the result with $\{\phi_j\}$ initialized from $\mathcal{N}(0, \sigma^2)$ and using the centered Fisher matrix is the most natural. However, when $D = 3, 5$, the results with $\{\psi_j\}$ initialized from $\mathcal{N}(2\pi/D, \sigma^2)$ show better convergence.

We have also found that using the uncentered Fisher matrix improves convergence for $D = 4$ where the centered Fisher matrix failed to find an appropriate optima. Our results suggest that the learning landscape of the VQEs with symmetry breaking layers is rugged especially when the parameters are not sufficient to describe the ground state accurately.

[1] F. Arute, K. Arya, R. Babbush, D. Bacon, J. C. Bardin, R. Barends, R. Biswas, S. Boixo, F. G. S. L. Brandao,

D. A. Buell, and et al., Quantum supremacy using a programmable superconducting processor, *Nature* **574**,

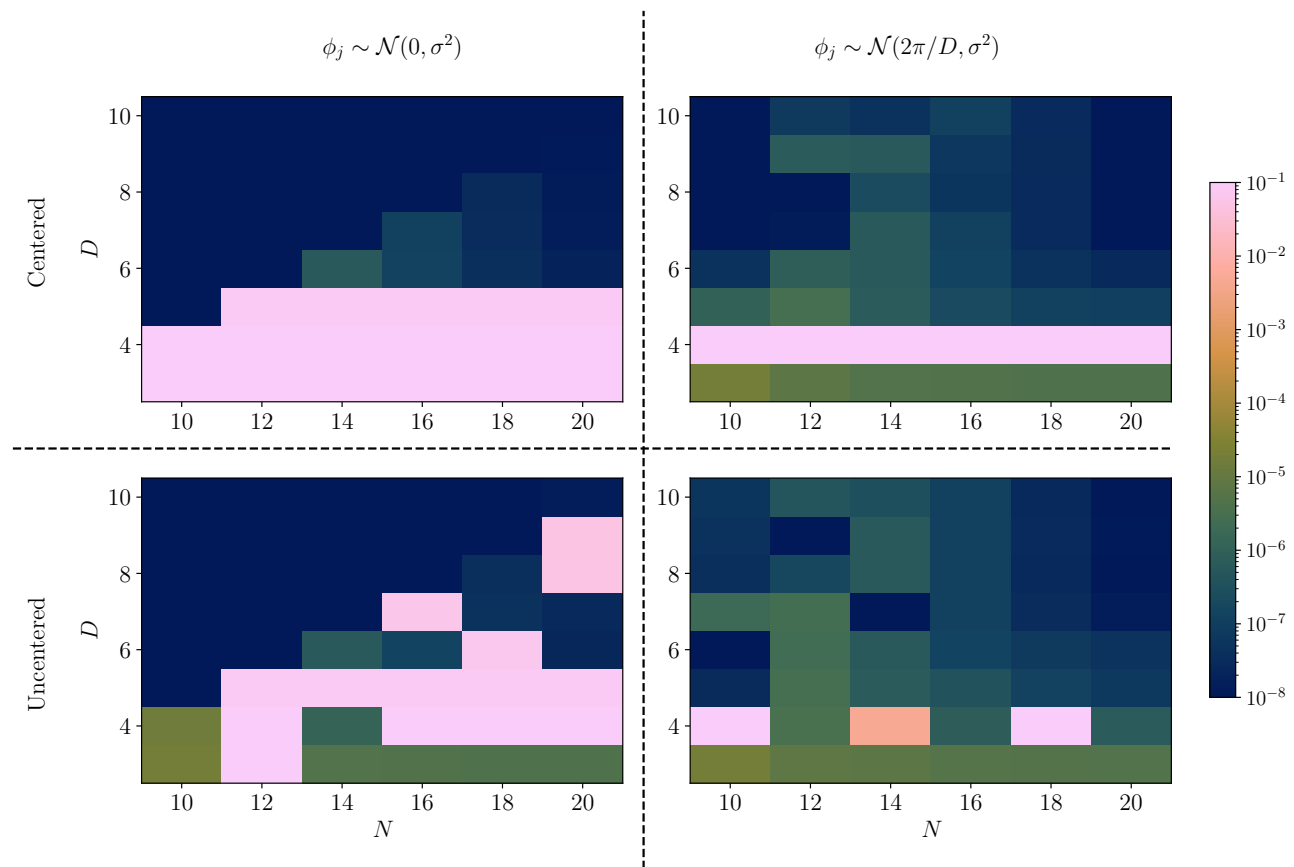


Figure 5. Converged normalized energies \tilde{E} for the TFI with different optimization set-ups. We have used the centered \mathcal{F}^c and uncentered Fisher matrix \mathcal{F}^{nc} for the upper and lower rows, respectively. The left and right columns show results from different initial values for the symmetry breaking layers. For each N and D , we have taken the best optimized energy from 12 independent VQE runs.

- 505–510 (2019).
- [2] J. Preskill, Quantum Computing in the NISQ era and beyond, *Quantum* **2**, 79 (2018).
- [3] A. Peruzzo, J. McClean, P. Shadbolt, M.-H. Yung, X.-Q. Zhou, P. J. Love, A. Aspuru-Guzik, and J. L. O’Brien, A variational eigenvalue solver on a photonic quantum processor, *Nature communications* **5**, 1 (2014).
- [4] J. R. McClean, J. Romero, R. Babbush, and A. Aspuru-Guzik, The theory of variational hybrid quantum-classical algorithms, *New Journal of Physics* **18**, 023023 (2016).
- [5] M. Cerezo, A. Arrasmith, R. Babbush, S. C. Benjamin, S. Endo, K. Fujii, J. R. McClean, K. Mitarai, X. Yuan, L. Cincio, *et al.*, Variational quantum algorithms, arXiv preprint arXiv:2012.09265 (2020).
- [6] S. Hadfield, Z. Wang, B. O’Gorman, E. G. Rieffel, D. Venturelli, and R. Biswas, From the quantum approximate optimization algorithm to a quantum alternating operator ansatz, *Algorithms* **12**, 34 (2019).
- [7] E. Farhi, J. Goldstone, and S. Gutmann, A quantum approximate optimization algorithm, arXiv preprint arXiv:1411.4028 (2014).
- [8] W. W. Ho and T. H. Hsieh, Efficient variational simulation of non-trivial quantum states, *SciPost Phys* **6**, 29 (2019).
- [9] D. Wierichs, C. Gogolin, and M. Kastoryano, Avoiding local minima in variational quantum eigensolvers with the natural gradient optimizer, *Physical Review Research* **2**, 043246 (2020).
- [10] R. Wiersema, C. Zhou, Y. de Sereville, J. F. Carrasquilla, Y. B. Kim, and H. Yuen, Exploring entanglement and optimization within the hamiltonian variational ansatz, *PRX Quantum* **1**, 020319 (2020).
- [11] S. Bravyi, A. Kliesch, R. Koenig, and E. Tang, Obstacles to variational quantum optimization from symmetry protection, *Physical Review Letters* **125**, 260505 (2020).
- [12] X. Chen, Z.-C. Gu, and X.-G. Wen, Complete classification of one-dimensional gapped quantum phases in interacting spin systems, *Physical Review B* **84**, 235128 (2011).
- [13] X. Chen, Z.-C. Gu, and X.-G. Wen, Classification of gapped symmetric phases in one-dimensional spin systems, *Physical Review B* **83**, 035107 (2011).
- [14] S. Bachmann, S. Michalakis, B. Nachtergaele, and R. Sims, Automorphic equivalence within gapped phases of quantum lattice systems, *Communications in Mathematical Physics* **309**, 835 (2012).
- [15] G. B. Mbeng, R. Fazio, and G. Santoro, Quantum annealing: A journey through digitalization, control, and hybrid quantum variational schemes, arXiv preprint arXiv:1906.08948 (2019).
- [16] S. McArdle, T. Jones, S. Endo, Y. Li, S. C. Benjamin,

- and X. Yuan, Variational ansatz-based quantum simulation of imaginary time evolution, *npj Quantum Information* **5**, 1 (2019).
- [17] J. Stokes, J. Izaac, N. Killoran, and G. Carleo, Quantum natural gradient, *Quantum* **4**, 269 (2020).
- [18] L. Hackl, T. Guaita, T. Shi, J. Haegeman, E. Demler, and J. I. Cirac, Geometry of variational methods: dynamics of closed quantum systems, *SciPost Phys.* **9**, 48 (2020).
- [19] C.-Y. Park and M. J. Kastoryano, Geometry of learning neural quantum states, *Physical Review Research* **2**, 10.1103/physrevresearch.2.023232 (2020).
- [20] G. Zonzo and S. M. Giampaolo, n-cluster models in a transverse magnetic field, *Journal of Statistical Mechanics: Theory and Experiment* **2018**, 063103 (2018).
- [21] W. Son, L. Amico, and V. Vedral, Topological order in 1d cluster state protected by symmetry, *Quantum Information Processing* **11**, 1961–1968 (2011).
- [22] B. Zeng, X. Chen, D.-L. Zhou, and X.-G. Wen, *Quantum information meets quantum matter* (Springer-Verlag New York, 2019).
- [23] C.-Y. Park, <https://github.com/chaeyeunpark/efficient-vqe-symmetry-breaking> (2021).